Article

Discovery Medicine 2026; 38(204): 95–105
https://doi.org/10.24976/Discov.Med.202638204.8

PPARα-Mediated Regulation of Ferroptosis as a Therapeutic Approach for Methotrexate-Induced Liver Injury

Yuxu You[1], Tianxiao Zhang[1], Lipin Huang[2], Han Zeng[1], Yu Chen[1,*]

[1]Department of Infectious Diseases, The People's Hospital of Cangnan, 325800 Wenzhou, Zhejiang, China
[2]Department of Cardiology, The People's Hospital of Cangnan, 325800 Wenzhou, Zhejiang, China
*Correspondence: 13646570945@163.com (Yu Chen)
Submitted: 6 November 2025 Revised: 28 November 2025 Accepted: 11 December 2025 Published: 20 January 2026

Background: Methotrexate (MTX) is widely used as a chemotherapeutic and immunosuppressive agent, but is frequently associated with hepatotoxicity. Ferroptosis, an iron-dependent form of cell death driven by lipid peroxidation, is increasingly recognized as a major contributor to drug-induced liver injury. Peroxisome proliferator-activated receptor α (PPARα) serves as a critical regulator of lipid metabolism and antioxidant defense. However, its role in MTX-induced hepatocyte ferroptosis remains unclear. This study aimed to determine whether PPARα modulates MTX-induced liver injury by regulating oxidative stress and ferroptosis *in vivo* and *in vitro*.

Methods: A mouse model of MTX-induced liver injury was established, and hepatic histopathology, serum biochemical parameters (alanine aminotransferase (ALT), aspartate aminotransferase (AST)), inflammatory cytokines (tumor necrosis factor α (TNF-α), interleukin-6 (IL-6)), oxidative stress markers (4-hydroxynonenal (4-HNE), malondialdehyde (MDA), superoxide dismutase (SOD), glutathione (GSH)), and ferroptosis-related proteins (glutathione peroxidase 4 (GPX4), solute carrier family 7 member 11 (SLC7A11), acyl-CoA synthetase long-chain family member 4 (ACSL4), arachidonate 15-lipoxygenase (ALOX15), transferrin receptor 1 (TFR1)) were assessed. PPAR-related signaling molecules (PPARα, PPARγ, and peroxisome proliferator-activated receptor gamma coactivator 1-α (PGC-1α)) were analyzed using Western blotting. *In vitro*, AML-12 hepatocytes were exposed to MTX with or without the PPARα agonist GW7647 to evaluate lipid peroxidation, antioxidant capacity, and ferroptosis markers.

Results: MTX treatment induced significant liver injury, characterized by hepatocellular swelling, vacuolization, elevated ALT/AST ($p < 0.05$), increased proinflammatory cytokines ($p < 0.05$), enhanced lipid peroxidation ($p < 0.05$), and reduced antioxidant capacity ($p < 0.05$). Ferroptosis-associated markers were significantly altered (decreased GPX4; increased ACSL4, ALOX15, and TFR1; $p < 0.05$). MTX also disrupted PPAR signaling (reduced PPARα and PGC-1α; increased PPARγ; $p < 0.05$). Activation of PPARα by GW7647 restored PGC-1α expression, enhanced antioxidant defenses (GPX4, SLC7A11, GSH, SOD; $p < 0.05$), suppressed ferroptosis-related lipid-remodeling enzymes ($p < 0.05$), and reduced lipid peroxidation ($p < 0.05$), thereby alleviating MTX-induced hepatocellular damage *in vivo* and *in vitro*.

Conclusion: PPARα activation mitigates MTX-induced liver injury by reprogramming lipid metabolism and enhancing antioxidant defenses, ultimately suppressing ferroptosis. These findings highlight the therapeutic potential of targeting the PPARα-ferroptosis pathway as an innovative strategy to counteract MTX-associated hepatotoxicity.

Keywords: MTX-induced liver injury; PPARα; ferroptosis; lipid peroxidation; antioxidant defense; GPX4

Introduction

Methotrexate (MTX) is a folate-based compound extensively used in the management of malignant tumors and autoimmune disorders [1,2]. Although clinically effective, MTX frequently induces liver toxicity in a dose-dependent manner, characterized by elevated serum transaminases, hepatic inflammation, and structural liver damage [3]. Recent studies indicate that oxidative stress and lipid peroxidation play pivotal roles in MTX-induced hepatocyte injury [4,5]. However, the precise mechanisms linking MTX exposure to hepatocyte death remain incompletely defined.

Ferroptosis, an iron-dependent form of regulated cell death triggered by uncontrolled lipid peroxidation, has recently been recognized as a key contributor to liver pathology, including drug-induced hepatotoxicity, ischemia-reperfusion injury, and nonalcoholic fatty liver disease [6–8]. This process is characterized by the accumulation of peroxidation-susceptible polyunsaturated fatty acid (PUFA) phospholipids, depletion of glutathione (GSH), and inactivation of glutathione peroxidase 4 (GPX4). Key enzymes such as acyl-CoA synthetase long-chain family member 4 (ACSL4) and arachidonate 15-lipoxygenase

(ALOX15) orchestrate the incorporation and oxygenation of PUFAs into phospholipids, thereby regulating cellular sensitivity to ferroptosis [9,10]. Accordingly, targeting ferroptosis has emerged as a promising strategy to alleviate hepatocyte injury and preserve liver function.

Peroxisome proliferator-activated receptor α (PPARα) is a nuclear receptor that serves as a master regulator of lipid metabolism and antioxidant defense [11–13]. PPARα activation reduces lipid accumulation, promotes fatty acid catabolism, and enhances the expression of antioxidant enzymes, all of which are critical components of the cellular ferroptosis-defense system [14–16]. Despite these established roles, the potential role of PPARα in modulating ferroptosis during MTX-induced liver injury has not been systematically investigated.

In the present study, we hypothesized that MTX-induced hepatotoxicity is mediated, at least in part, by dysregulated ferroptosis and disruption of PPARα signaling. Using a combination of *in vivo* MTX-induced liver injury models and *in vitro* hepatocyte experiments, we aimed to determine whether activation of PPARα can reprogram lipid metabolism, enhance antioxidant defenses, and suppress ferroptotic pathways to protect hepatocytes from MTX-mediated damage. Our findings provide new insights into the mechanistic relationship between PPARα signaling and ferroptosis in drug-induced hepatotoxicity, offering potential therapeutic strategies for clinical intervention.

Materials and Methods

Animals Model

Male C57BL/6 mice (6–8 weeks old, SPF grade; total n = 42) were purchased from Beijing Speifu Biotechnology Co., Ltd. (Beijing, China). All animals, weighing 18–22 g, were acclimated for one week under standard laboratory conditions (22–25 °C, 12 h light/dark cycle) with *ad libitum* access to food and water. To evaluate MTX-induced liver injury, mice were randomly assigned to three groups (n = 6 per group) and received saline (control), low-dose MTX (2 mg/kg, intraperitoneally; HY-14519, MedChemExpress, CA, USA), or high-dose MTX (20 mg/kg, intraperitoneally). Body weight and general health were monitored throughout the study. The dosing regimen was selected based on previous reports [17,18]. MTX was administered as a single intraperitoneal injection, and three days later, mice were euthanized. Euthanasia was performed using an overdose of pentobarbital sodium (150 mg/kg, intraperitoneally), followed by cervical dislocation to ensure complete euthanasia. Liver tissues and blood samples were subsequently collected.

To examine the protective effects of PPARα overexpression against MTX-induced hepatotoxicity, adeno-associated virus serotype 9 (AAV9) vectors carrying either PPARα (AAV9-PPARα; Genechem, Shanghai, China) or an empty vector (AAV9-NC) were administered via tail vein injection to half of the mice (n = 12). All animals used for AAV9 experiments were independent from the first cohort, and the AAV9-related study was performed as a separate batch to avoid cross-interference. Viral preparations were provided at a titer of 1×10^{12} viral genomes (vg)/mL, and each mouse received 100 µL via the tail vein. The construct contained full-length mouse PPARα (NM_011144.6) cDNA driven by a CMV promoter and packaged into an AAV9 capsid. Four weeks after vector delivery, mice were randomly assigned to four experimental groups (n = 6 per group) for evaluation of MTX-induced liver injury: control mice with AAV9 empty vector (Con + WT), control mice with AAV9-PPARα (Con + OE), MTX-treated mice with AAV9 empty vector (MTX + WT), and MTX-treated mice with AAV9-PPARα (MTX + OE). MTX (20 mg/kg, intraperitoneally) was administered using the standard dose for inducing acute liver injury in AAV-modified mouse models. Three days after MTX injection, mice were sacrificed for the collection of liver tissues and blood samples for histological, biochemical, and molecular analyses.

Cell Culture and Treatment

AML-12 mouse hepatocytes were obtained from Procell (CL-0602, Wuhan, China) and cultured in DMEM/F12 medium (11320033, Gibco, MA, USA) supplemented with 10% fetal bovine serum (FBS; A5670701, Gibco, MA, USA) and 1% penicillin-streptomycin (15140122, Gibco, MA, USA) at 37 °C incubators containing 5% CO_2. Cells were seeded in 6-well or 96-well plates, depending on experimental requirements.

For *in vitro* assays, AML-12 cells (a mouse hepatocyte line exhibiting epithelial-like morphology with polygonal cell shape and distinct cell borders) were confirmed to be free of mycoplasma contamination via routine PCR-based screening before the experiments. AML-12 cells were treated with MTX (30 µM) for 24 hours with or without 6-hour pretreatment with GW7647 (5 µM; ab141124, Abcam, UK). Control cells were exposed to vehicle (DMSO). The concentrations of MTX and GW7647 were selected based on previous studies [18,19]. After treatment, cells were harvested for assessment of ferroptosis markers, oxidative stress indicators, and PPAR signaling proteins using Western blotting or biochemical assays.

Histological Analysis

Liver tissues were harvested, fixed in 10% formalin, embedded in paraffin, and sectioned at 4 µm. For hematoxylin and eosin (H&E) staining, sections were deparaffinized in xylene, rehydrated through a graded ethanol series, and stained with a hematoxylin solution (G1120, Solarbio, Beijing, China) for 5 min, followed by differentiation in 1% acid alcohol and bluing in running tap water. Slides were then counterstained with eosin solution (G1100, Solarbio, Beijing, China) for 2 min, dehydrated, cleared, and mounted using a neutral resin mounting medium (G8590,

Solarbio, Beijing, China). Representative images were captured using a light microscope (AH-2, Olympus, Tokyo, Japan).

Biochemical Analyses

At the end of the experiment, mice were euthanized by intraperitoneal injection of sodium pentobarbital (150 mg/kg). After cessation of respiration, cardiac puncture was performed using a 1 mL syringe with a 25G needle to obtain whole blood, which was allowed to clot for 30 min at room temperature and subsequently centrifuged at 3000 rpm for 10 min at 4 °C. Serum was collected and stored at –80 °C until analysis. Serum alanine aminotransferase (ALT) and aspartate aminotransferase (AST) levels were determined using commercial assay kits (C009-2-1, C010-2-1; Nanjing Jiancheng Bioengineering Institute, Nanjing, China) according to the manufacturer's instructions, and absorbance was detected at 510 nm using a microplate reader (SpectraMax i3x, Molecular Devices, CA, USA). Proinflammatory cytokines, including tumor necrosis factor α (TNF-α) and interleukin-6 (IL-6), were quantified using enzyme-linked immunosorbent assay (ELISA) kits (MTA00B, M6000B; R&D Systems, MN, USA), with absorbance recorded at 450 nm and reference 570 nm. Hepatic and cellular oxidative stress were evaluated by quantifying 4-hydroxynonenal (4-HNE), malondialdehyde (MDA), superoxide dismutase (SOD), and GSH using commercial kits (H268-1-1, A003-1-2, A001-3-2, A006-2-1, Nanjing Jiancheng Bioengineering Institute, Nanjing, China) following the manufacturers' protocols. Detection wavelengths were 450 nm for 4-HNE, 532 nm for MDA, 550 nm for SOD, and 405 nm for GSH.

Western Blot Analysis

Protein extracts from liver tissues and AML-12 cells were prepared using RIPA lysis buffer (P0013B, Beyotime, Shanghai, China). Protein concentration was measured using a BCA assay (23227, Thermo Scientific, MA, USA). Equal amounts of protein were separated by SDS-PAGE and transferred to PVDF membranes. Membranes were blocked with 5% non-fat milk and incubated overnight at 4 °C with primary antibodies against GPX4 (1:500, 30388-1-AP, Proteintech, Wuhan, China), solute carrier family 7 member 11 (SLC7A11) (1:1000, 32384-1-AP, Proteintech, Wuhan, China), acyl-CoA synthetase long-chain family member 4 (ACSL4) (1:5000, 22401-1-AP, Proteintech, Wuhan, China), ALOX15 (1:500, 13286-1-AP, Proteintech, Wuhan, China), transferrin receptor 1 (TFR1) (1:2000, 84766-4-RR, Proteintech, Wuhan, China), PPARα (1:1000, 15540-1-AP, Proteintech, Wuhan, China), PPARγ (1:1000, 16643-1-AP, Proteintech, Wuhan, China), and peroxisome proliferator-activated receptor gamma coactivator 1-α (PGC-1α) (1:5000, 66369-1-Ig, Proteintech, Wuhan, China) at recommended dilutions. Membranes were incubated with HRP-conjugated secondary antibodies (1:2000; SA00001-1 or SA00001-2, Proteintech, Wuhan, China). Protein bands were visualized using ECL reagent (PE0010, Solarbio, Beijing, China) and imaged with a ChemiDoc MP 1708280 Imaging System (Bio-Rad, CA, USA). Band intensities were quantified using ImageJ software (version 1.54i, National Institutes of Health, Bethesda, MD, USA).

Statistical Analysis

All data are presented as mean $\pm$ standard deviation (SD). Statistical analyses were performed using GraphPad Prism 9.5 (GraphPad Software, San Diego, CA, USA). Prior to hypothesis testing, data were assessed for normality using the Shapiro-Wilk test and for homogeneity of variance using Levene's test. For comparisons between two groups, normally distributed data with equal variances were analyzed using Student's *t*-test. For comparisons among multiple groups, one-way ANOVA was applied, followed by Tukey's post hoc test, which adjusts for multiple pairwise comparisons. When normality or homoscedasticity assumptions were not met, nonparametric tests (Mann-Whitney U test or Kruskal-Wallis test with Dunn's post hoc correction) were employed. A two-tailed $p < 0.05$ was considered statistically significant.

Results

Establishment of the MTX-Induced Mouse Model and Alterations in PPAR Signaling

To evaluate how MTX influences hepatic PPAR signaling, we established a murine model that mimics MTX-induced liver injury (Fig. 1A). H&E staining revealed characteristic histopathological alterations, including hepatocellular swelling and vacuolization, with occasional infiltration of inflammatory cells (Fig. 1B). Serum biochemical markers (ALT and AST) were significantly elevated (Fig. 1C,D; $p < 0.05$), confirming impaired liver function, while proinflammatory cytokines (TNF-α and IL-6) were markedly increased (Fig. 1E,F; $p < 0.05$). In parallel, oxidative stress was exacerbated, as indicated by increased 4-HNE and MDA levels ($p < 0.05$), along with reduced antioxidant capacity (SOD and GSH; $p < 0.05$) (Fig. 1G–J). Moreover, ferroptosis-associated proteins demonstrated a significant decrease in GPX4 expression, together with elevated ACSL4 and TFR1 levels (Fig. 1K–N; $p < 0.05$), suggesting activation of ferroptosis in MTX-treated mice. Notably, Western blot analysis revealed that MTX treatment dysregulated PPAR signaling: PPARα and PGC-1α expression were significantly downregulated, whereas PPARγ expression was increased (Fig. 1O–R; $p < 0.05$). Collectively, these findings suggest that MTX-induced hepatotoxicity involves alterations in PPAR signaling pathways, which may contribute to enhanced ferroptosis.

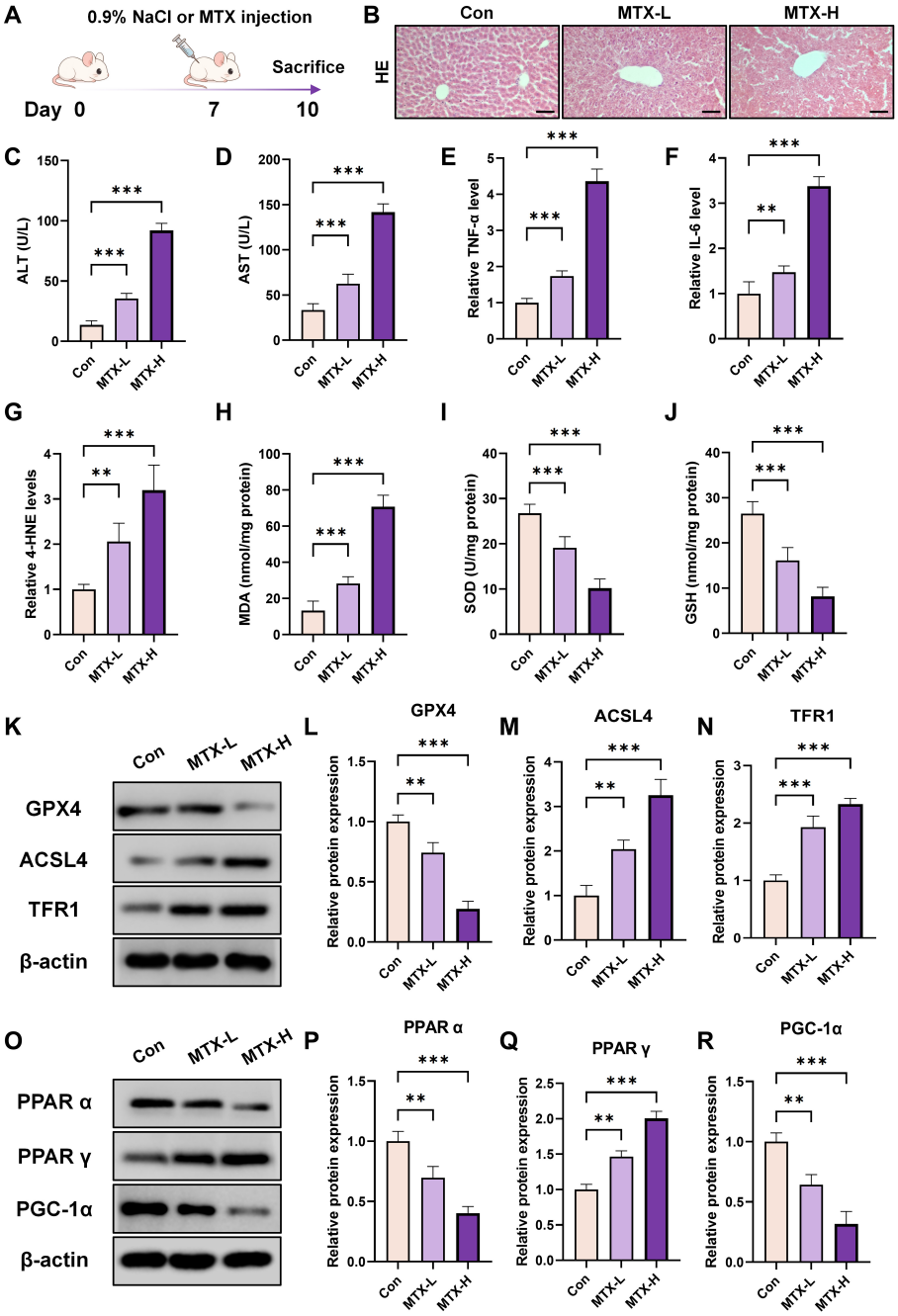

Fig. 1. Establishment of the MTX-induced mouse model of liver injury. (A) Schematic illustration of the experimental design for MTX-induced liver injury in mice. (B) Representative H&E staining of liver tissue (scale bar = 50 μm). (C,D) Serum levels of ALT and AST. (E,F) Relative serum levels of TNF-α and IL-6 measured by ELISA. (G,H) Relative serum levels of 4-HNE and MDA. (I,J) Serum levels of SOD and GSH. (K–N) Representative Western blot images and quantification of ferroptosis-related markers (GPX4, ACSL4, TFR1) in mouse liver tissue. (O–R) Representative Western blot images and quantification of PPAR signaling proteins (PPARα, PPARγ, and PGC-1α) in mouse liver tissue. Data are presented as mean ± SD (n = 6). $^{**}p < 0.01$, $^{***}p < 0.001$ (vs. control). MTX, Methotrexate; H&E, hematoxylin and eosin; ALT, alanine aminotransferase; AST, aspartate aminotransferase; TNF-α, tumor necrosis factor α; IL-6, interleukin-6; ELISA, enzyme-linked immunosorbent assay; 4-HNE, 4-hydroxynonenal; MDA, malondialdehyde; SOD, superoxide dismutase; GSH, glutathione; GPX4, glutathione peroxidase 4; ACSL4, acyl-CoA synthetase long-chain family member 4; TFR1, transferrin receptor 1; PPAR, peroxisome proliferator-activated receptor; PGC-1α, peroxisome proliferator-activated receptor gamma coactivator 1-α.

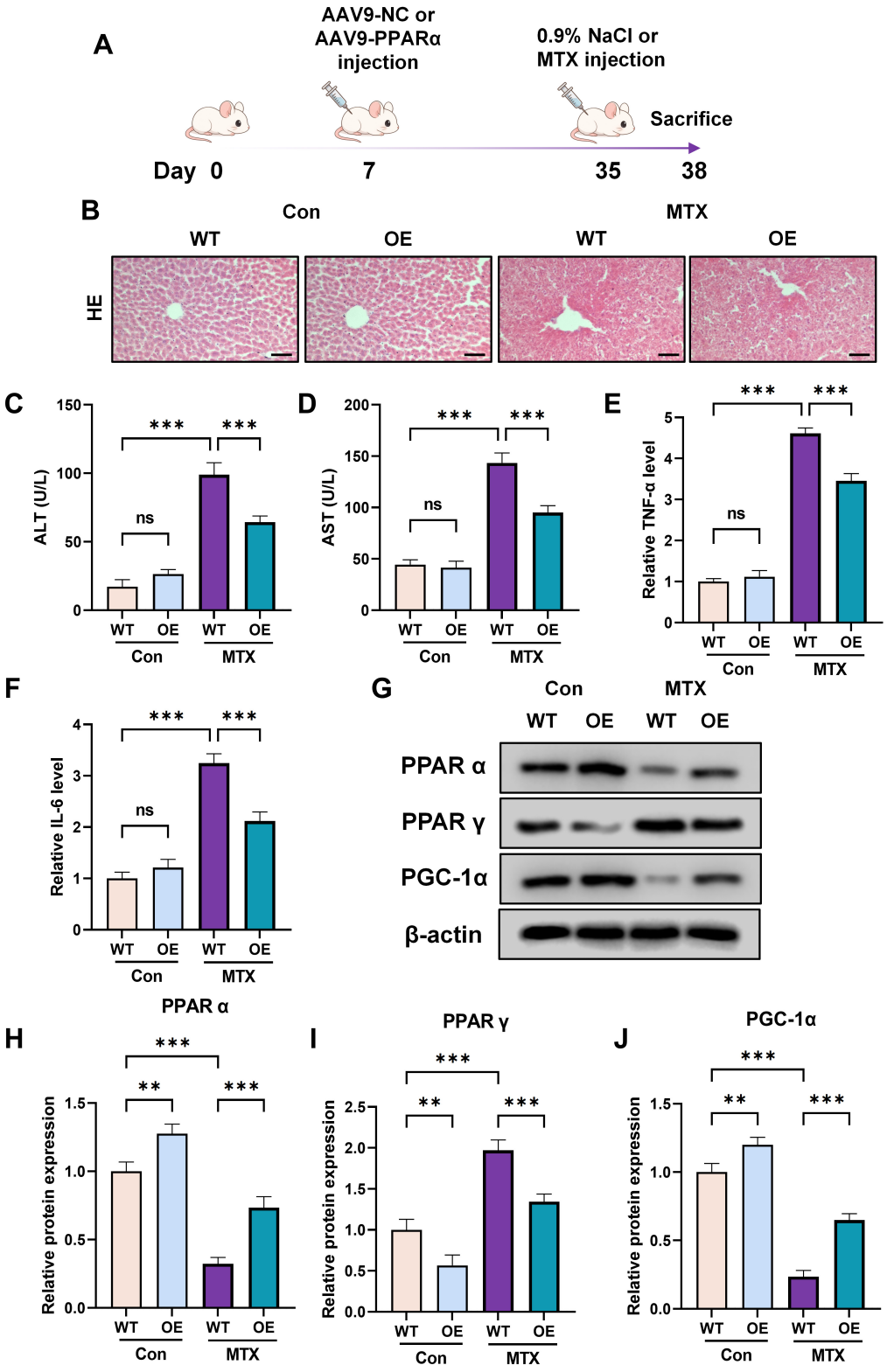

Fig. 2. Effect of PPARα overexpression on MTX-induced liver injury. (A) Schematic diagram of PPARα overexpression in mice. (B) Representative H&E staining images of liver tissue (scale bar = 50 µm). (C,D) Serum ALT and AST levels. (E,F) Relative serum levels of TNF-α and IL-6 determined by ELISA. (G–J) Representative Western blot images and quantitative analysis of PPARα, PPARγ, and PGC-1α expression in mouse liver tissue. Data are presented as mean ± SD (n = 6). ns, not significant ($p > 0.05$); $^{**}p < 0.01$, $^{***}p < 0.001$.

PPARα Overexpression Alleviates MTX-Induced Liver Injury

To further elucidate the role of PPARα in MTX-induced hepatotoxicity, PPARα-overexpressing mice were generated (Fig. 2A). H&E staining demonstrated that PPARα overexpression markedly attenuated MTX-induced histopathological alterations, including hepatocyte necrosis and vacuolization, with minimal inflammatory infiltration observed (Fig. 2B). In MTX-treated PPARα overexpression group, serum ALT and AST levels were significantly reduced (Fig. 2C,D; $p < 0.05$), and inflammatory cytokines (TNF-α and IL-6) were similarly decreased ($p < 0.05$) compared with MTX-treated controls (Fig. 2E,F). Western blot analysis confirmed successful upregulation of PPARα, which was accompanied by restored PGC-1α expression and a concomitant reduction in PPARγ levels in the MTX-treated PPARα overexpression group (Fig. 2G–J; $p < 0.05$). These findings indicate that PPARα overexpression confers protection against MTX-induced liver injury.

PPARα Overexpression Reduces Ferroptosis in MTX-Treated Mice

To elucidate how PPARα confers protection against MTX-induced liver injury, markers of oxidative stress and ferroptosis were assessed. In the MTX-treated PPARα overexpression group, PPARα overexpression significantly reduced serum 4-HNE and MDA levels while enhancing antioxidant defenses, as indicated by increased SOD and GSH levels (Fig. 3A–D; $p < 0.05$). Moreover, in this group, PPARα overexpression elevated GPX4 and SLC7A11 expression, while downregulating ACSL4, ALOX15, and TFR1 levels (Fig. 3E–J; $p < 0.05$). These findings indicate that PPARα mitigates MTX-induced oxidative stress and suppresses ferroptosis in mouse liver tissue.

PPARα Activation by GW7647 Attenuates Ferroptosis in AML-12 Cells

To further validate the protective role of PPARα at the cellular level, AML-12 hepatocytes were treated with the PPARα agonist GW7647. Western blot analysis confirmed that, in the MTX-treated group, GW7647 treatment enhanced PPARα expression, restored PGC-1α levels, and reduced PPARγ expression (Fig. 4A–D; $p < 0.05$). Consistent with the *in vivo* results, in the MTX-treated group, GW7647 treatment reduced the intracellular accumulation of 4-HNE and MDA while significantly increasing GSH levels (Fig. 4E–G; $p < 0.05$). Moreover, ferroptosis-related proteins showed changes similar to those observed in liver tissue: GPX4 and SLC7A11 were upregulated, whereas ACSL4, ALOX15, and TFR1 were downregulated (Fig. 4H–M; $p < 0.05$). These findings demonstrate that pharmacological activation of PPARα by GW7647 effectively alleviates MTX-induced ferroptosis both *in vivo* and *in vitro*.

Discussion

In this study, we demonstrate that MTX-induced liver injury is associated with the dysregulation of PPAR signaling and the activation of ferroptotic pathways. Furthermore, we show that restoring PPARα activity, either through genetic overexpression *in vivo* or pharmacological activation (GW7647) *in vitro*, attenuates MTX-induced hepatocellular damage. MTX-treated liver tissues exhibited histological injury, elevated ALT/AST and proinflammatory cytokines, increased lipid peroxidation (4-HNE, MDA) and reduced antioxidant capacity (SOD, GSH). Consistent with earlier reports, MTX promotes oxidative stress, lipid peroxidation, and ferroptosis in hepatocytes [20–22]. Concurrently, ferroptosis markers, including decreased GPX4 expression, elevated ACSL4 levels, and increased TFR1 expression, were observed, together with disruptions in PPAR signaling characterized by reduced PPARα and PGC-1α expression and increased PPARγ activity. Comparable perturbations in PPAR signaling under stress conditions have been documented in other models of drug-induced or disease-associated liver injury [23–25]. Restoration of PPARα activity reversed these changes: PPARα upregulation or activation restored PGC-1α, increased GPX4 and SLC7A11, and reduced ACSL4, ALOX15, and TFR1, thereby lowering lipid peroxidation biomarkers in both liver tissue and in AML-12 cells. Collectively, these data indicate that PPARα protects against MTX hepatotoxicity by suppressing ferroptosis through coordinated regulation of lipid metabolism and antioxidant defenses.

One of the central mechanisms by which PPARα activation reduced ferroptotic signaling in our models involves reprogramming of lipid metabolic pathways that determine the abundance and composition of phospholipid substrates susceptible to peroxidation. MTX increased expression of ACSL4 and ALOX15, enzymes that activate long-chain PUFAs for membrane incorporation, esterify PUFAs into phospholipids, and catalyze oxygenation of PUFA-containing lipids, thereby generating a biochemical milieu conducive to ferroptotic lipid peroxidation. Previous studies have demonstrated that ACSL4 and ALOX15 are essential determinants of ferroptosis sensitivity due to their role in PUFA-phospholipid remodeling [26–28]. PPARα restoration markedly suppressed ACSL4 and ALOX15, which would (a) reduce the pool of PUFA-containing phospholipids available for peroxidation and (b) lower enzyme-driven lipid oxidation.

In parallel, the MTX-induced elevation of TFR1 suggests an enhanced import of labile iron, supplying Fe^{2+} required to drive lipid peroxidation and trigger ferroptotic cell death. As a principal regulator of cellular iron entry, TFR1 was suppressed upon PPARα activation, which likely reduces intracellular free iron levels, thereby decreasing Fenton reaction-mediated ROS generation and further protecting hepatocytes from ferroptosis. These findings suggest

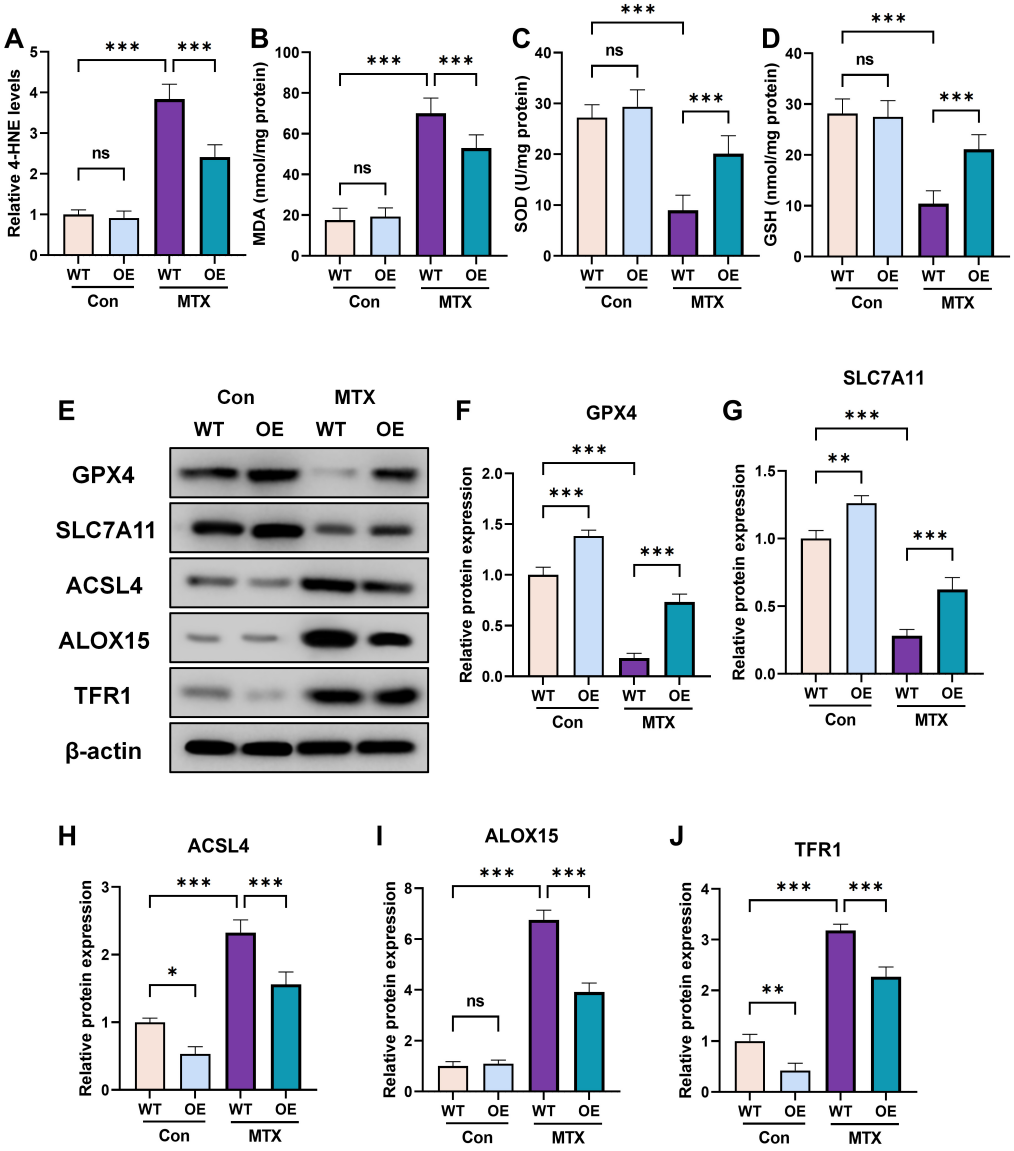

Fig. 3. Effects of PPARα overexpression on oxidative stress and ferroptosis in MTX-treated mice. (A,B) Relative serum levels of 4-HNE and MDA. (C,D) Serum levels of SOD and GSH. (E–J) Representative Western blot images and quantitative analysis of ferroptosis-related markers (GPX4, SLC7A11, ACSL4, ALOX15, TFR1) in mouse liver tissue. Data are presented as mean ± SD (n = 6). ns, not significant ($p > 0.05$); $^{*}p < 0.05$, $^{**}p < 0.01$, $^{***}p < 0.001$. SLC7A11, solute carrier family 7 member 11; ALOX15, arachidonate 15-lipoxygenase.

that PPARα not only modulates lipid substrate availability and oxidation but also indirectly regulates iron-dependent pro-ferroptotic signals.

Concurrently, we observed recovery of PGC-1α expression following PPARα activation. As a pivotal transcriptional coactivator regulating mitochondrial biogenesis and fatty acid catabolism, its restoration suggests enhanced mitochondrial fatty acid (FA) oxidation and improved clearance of surplus fatty acids that would otherwise serve as substrates for lipid peroxidation. This observation aligns with previous reports demonstrating that activation of the PPARα–PGC-1α axis enhances mitochondrial oxidative metabolism and protects against hepatic lipid accumulation and oxidative stress [29–31]. Thus, through the suppression of ACSL4 and ALOX15, restoration of PGC-1α-dependent metabolic homeostasis, and the reduction of iron influx via TFR1 downregulation, PPARα activity decreases substrate availability for ferroptotic lipid peroxidation, and consequently reduces hepatocyte vulnerability to ferroptotic injury.

A second, complementary mechanism involves enhancement of cellular antioxidant defenses. MTX treatment resulted in a marked depletion of antioxidant indicators (SOD, GSH) and downregulation of GPX4, the essential enzyme that detoxifies phospholipid hydroperoxides into inert lipid alcohols. Activation or overexpression of

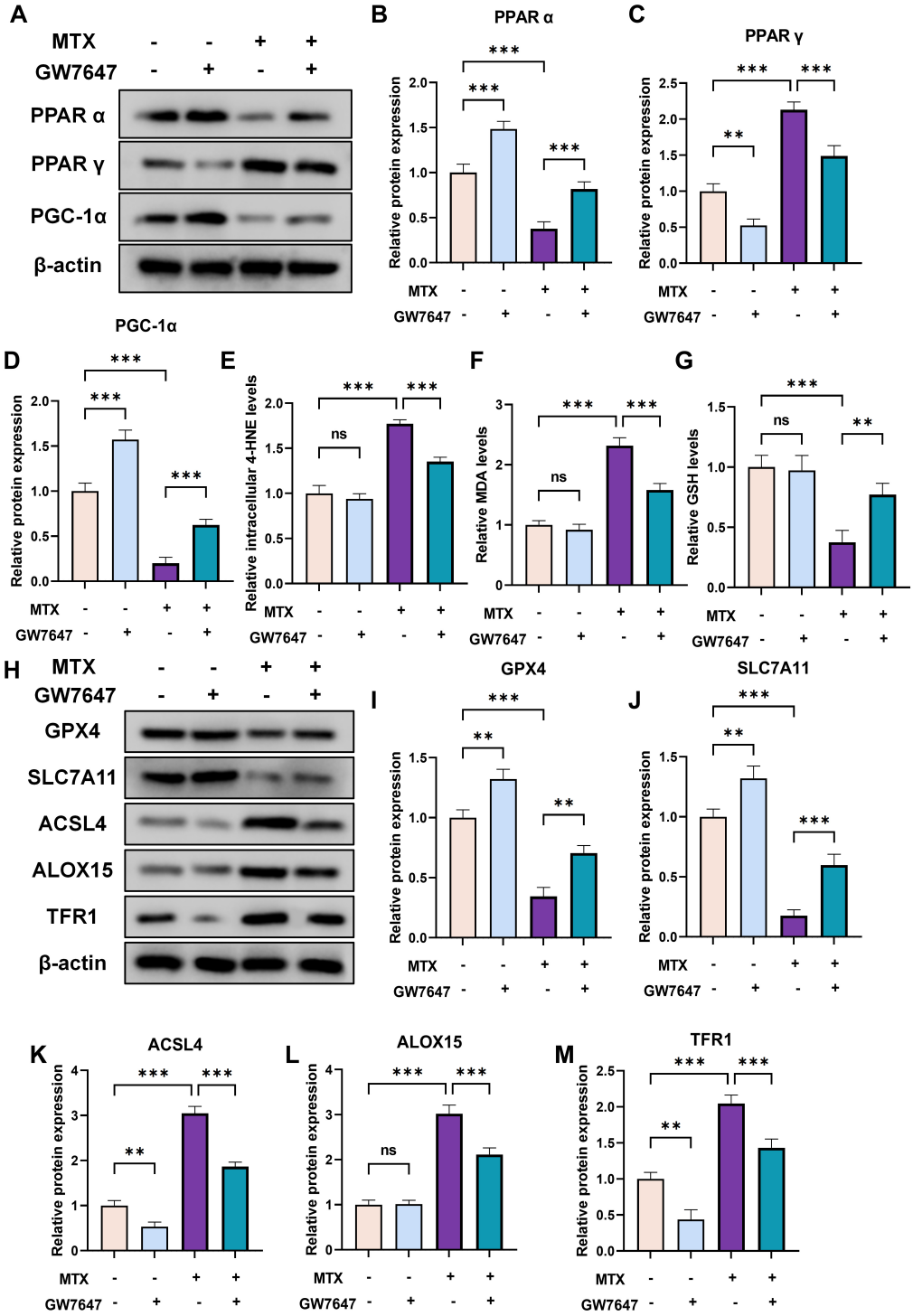

Fig. 4. Effects of PPARα activation by GW7647 on ferroptosis in AML-12 hepatocytes. (A–D) Representative Western blot images and quantitative analysis of PPARα, PPARγ, and PGC-1α in AML-12 cells. (E,F) Relative intracellular levels of 4-HNE and MDA. (G) Intracellular GSH levels. (H–M) Representative Western blot images and quantitative analysis of ferroptosis-related markers (GPX4, SLC7A11, ACSL4, ALOX15, TFR1) in AML-12 cells. Data are presented as mean ± SD (n = 3). ns, not significant ($p > 0.05$); $^{**}p < 0.01$, $^{***}p < 0.001$.

PPARα restored intracellular GSH and SOD activity while elevating GPX4 and SLC7A11 expression. As SLC7A11 mediates cystine uptake for GSH synthesis and GPX4 requires GSH as a cofactor to detoxify lipid peroxides, coordinated upregulation of these proteins reconstitutes the GSH-dependent anti-ferroptotic system. Additionally, PPARα may promote antioxidant capacity directly through the transcriptional regulation of redox-responsive genes or indi-

rectly via metabolic remodeling that reduced ROS production; the present data show the functional consequence—reduced lipid peroxidation (lower 4-HNE/MDA) and increased GSH/antioxidant enzyme activity—consistent with an enhanced detoxification capacity that antagonizes ferropto.

Ferroptosis is driven by the convergence of (1) the abundance of peroxidation-prone phospholipid substrates, (2) the availability of catalytically active labile Fe^{2+}, and (3) insufficient detoxification of lipid peroxides. Our findings indicate that PPARα activity disrupts this feed-forward cycle at multiple mechanistic levels. By suppressing ACSL4 and ALOX15, PPARα reduces the pool of PUFA-enriched phospholipids and limits enzymatic lipid oxygenation. Simultaneously, by upregulating SLC7A11 and GPX4 and replenishing antioxidant reserves (GSH, SOD), PPARα increases the cellular threshold required for the accumulation of lethal lipid hydroperoxides. The combined effect is the generation of fewer lipid peroxides and improved clearance of those generated, thereby restricting the capacity of labile Fe^{2+} to catalyze lipid radical chain reactions and halting the biochemical cascade that leads to ferroptotic cell death. Collectively, these mechanisms translate into robust protection of hepatocytes from MTX-induced injury, as evidenced by improved histopathology and improved serum biomarker profiles.

Our results suggest that modulation of PPARα represents a promising strategy to mitigate MTX-induced liver injury. Pharmacological activation of PPARα (we used GW7647 *in vitro*) reproduced the protective effects observed with genetic upregulation, supporting its translational potential. Clinically used PPARα agonists (such as fibrates) or newly developed selective activators may therefore be repurposed to prevent or treat drug-induced ferroptotic liver injury. However, species-specific differences in PPAR biology and the complexity of PPAR family signaling (including the MTX-associated increase in PPARγ) warrant careful preclinical dose-finding, safety assessment, and evaluation of potential off-target metabolic effects before clinical translation. Moreover, the external validity of our findings should be interpreted with caution, as the acute high-dose MTX model used in this study differs from the chronic low-dose regimens commonly applied in clinical settings. Acute and chronic MTX hepatotoxicity may involve overlapping yet distinct mechanisms. Thus, future studies employing long-term MTX exposure or alternative clinically relevant dosing paradigms will be required to further validate the translational applicability of PPARα-targeted therapeutic strategies. Additionally, although our biochemical and molecular findings strongly support ferroptotic involvement, we did not perform reversible rescue experiments using established ferroptosis inhibitors such as ferrostatin-1 or Liproxstatin-1. Incorporating these pharmacological rescue approaches into future work will help establish the contribution of ferroptosis to MTX-induced liver injury more definitively and further clarify how PPARα activation modulates this process.

Conclusion

This study demonstrates that activation or overexpression of PPARα confers significant protection against MTX-induced liver injury by suppressing ferroptosis. Mechanistically, PPARα remodels lipid metabolism by downregulating ACSL4 and ALOX15, thereby restoring PGC-1α-associated lipid metabolic homeostasis and reducing the availability of peroxidation-prone phospholipids. In parallel, PPARα strengthens the antioxidant defense network via increased expression of GPX4 and SLC7A11, effectively limiting lipid peroxidation and labile Fe^{2+}-driven ferroptotic cascades. Overall, our results position PPARα as a central modulator of ferroptosis and indicate that targeted activation of PPARα could be leveraged to counter MTX-induced liver injury.

Availability of Data and Materials

The data that support the findings of this study are available from the corresponding author upon reasonable request.

Author Contributions

YY, TZ and YC designed the research study; YY, LH, and HZ performed the experiments and collected the data; TZ, HZ and YC analyzed and interpreted the data; YY and TZ drafted the manuscript; LH, HZ, and YC critically revised the manuscript for important intellectual content. YC supervised the project and provided overall guidance. All authors have read and approved the final version of the manuscript. All authors have participated sufficiently in the work to take public responsibility for appropriate portions of the content and agreed to be accountable for all aspects of the work in ensuring that questions related to its accuracy or integrity are appropriately investigated and resolved.

Ethics Approval and Consent to Participate

All animal experiments were approved and conducted in accordance with the guidelines established by the Institutional Animal Care Committee of the People's Hospital of Cangnan (Approval No. 2024026).

Acknowledgment

Not applicable.

Funding

This research was funded by the Science and Technology Program of Wenzhou (No. Y20240260).

Conflict of Interest

The authors declare no conflict of interest.

References

[1] Hamed KM, Dighriri IM, Baomar AF, Alharthy BT, Alenazi FE, Alali GH, *et al*. Overview of Methotrexate Toxicity: A Comprehensive Literature Review. Cureus. 2022; 14: e29518. https://doi.org/10.7759/cureus.29518.

[2] Solipuram V, Mohan A, Patel R, Ni R. Effect of janus kinase inhibitors and methotrexate combination on malignancy in patients with rheumatoid arthritis: a systematic review and meta-analysis of randomized controlled trials. Auto-Immunity Highlights. 2021; 12: 8. https://doi.org/10.1186/s13317-021-00153-5.

[3] Ezhilarasan D. Hepatotoxic potentials of methotrexate: Understanding the possible toxicological molecular mechanisms. Toxicology. 2021; 458: 152840. https://doi.org/10.1016/j.tox.2021.152840.

[4] Abdallah N, Amer ME, Amer MA, El-Missiry MA, Othman AI. Melatonin mitigated methotrexate-induced hepatotoxicity through interrelated biological processes. Molecular Biology Reports. 2024; 51: 833. https://doi.org/10.1007/s11033-024-09792-z.

[5] Azadian R, Mohammadalipour A, Memarzadeh MR, Hashemnia M, Aarabi MH. Examining hepatoprotective effects of astaxanthin against methotrexate-induced hepatotoxicity in rats through modulation of Nrf2/HO-1 pathway genes. Naunyn-Schmiedeberg's Archives of Pharmacology. 2024; 397: 371–380. https://doi.org/10.1007/s00210-023-02581-8.

[6] Zeng L, Jin X, Xiao QA, Jiang W, Han S, Chao J, *et al*. Ferroptosis: action and mechanism of chemical/drug-induced liver injury. Drug and Chemical Toxicology. 2024; 47: 1300–1311. https://doi.org/10.1080/01480545.2023.2295230.

[7] Luan X, Chen P, Miao L, Yuan X, Yu C, Di G. Ferroptosis in organ ischemia-reperfusion injuries: recent advancements and strategies. Molecular and Cellular Biochemistry. 2025; 480: 19–41. https://doi.org/10.1007/s11010-024-04978-2.

[8] Peleman C, Francque S, Berghe TV. Emerging role of ferroptosis in metabolic dysfunction-associated steatotic liver disease: revisiting hepatic lipid peroxidation. eBioMedicine. 2024; 102: 105088. https://doi.org/10.1016/j.ebiom.2024.105088.

[9] Jiang Y, Zhang M, Sun M. ACSL4 at the helm of the lipid peroxidation ship: a deep-sea exploration towards ferroptosis. Frontiers in Pharmacology. 2025; 16: 1594419. https://doi.org/10.3389/fphar.2025.1594419.

[10] Zhang S, Guo L, Tao R, Liu S. Ferroptosis-targeting drugs in breast cancer. Journal of Drug Targeting. 2025; 33: 42–59. https://doi.org/10.1080/1061186X.2024.2399181.

[11] Van den Bossche V, Vignau J, Vigneron E, Rizzi I, Zaryouh H, Wouters A, *et al*. PPARα-mediated lipid metabolism reprogramming supports anti-EGFR therapy resistance in head and neck squamous cell carcinoma. Nature Communications. 2025; 16: 1237. https://doi.org/10.1038/s41467-025-56675-3.

[12] Wang X, Wang J, Ying C, Xing Y, Su X, Men K. Fenofibrate alleviates NAFLD by enhancing the PPARα/PGC-1α signaling pathway coupling mitochondrial function. BMC Pharmacology & Toxicology. 2024; 25: 7. https://doi.org/10.1186/s40360-023-00730-6.

[13] Liu Y, Wang F, Xu H, Wang H, Lu M, Cheng L. Ginkgolide B attenuates hyperlipidemia by restoring sphingolipid homeostasis and activating PPARα and Nrf2 pathways. Scientific Reports. 2025; 15: 28774. https://doi.org/10.1038/s41598-025-14626-4.

[14] Dong J, Li M, Peng R, Zhang Y, Qiao Z, Sun N. ACACA reduces lipid accumulation through dual regulation of lipid metabolism and mitochondrial function via AMPK- PPARα- CPT1A axis. Journal of Translational Medicine. 2024; 22: 196. https://doi.org/10.1186/s12967-024-04942-0.

[15] Yang H, Ran S, Zhou Y, Shi Q, Yu J, Wang W, *et al*. Exposure to Succinate Leads to Steatosis in Non-Obese Non-Alcoholic Fatty Liver Disease by Inhibiting AMPK/PPARα/FGF21-Dependent Fatty Acid Oxidation. Journal of Agricultural and Food Chemistry. 2024; 72: 21052–21064. https://doi.org/10.1021/acs.jafc.4c05671.

[16] Feng Y, Wang H, Hu Y, Zhang X, Miao X, Li Z, *et al*. Hederagenin ameliorates ferroptosis-induced damage by regulating PPARα/Nrf2/GPX4 signaling pathway in HT22 cells: An in vitro and in silico study. Bioorganic Chemistry. 2025; 155: 108119. https://doi.org/10.1016/j.bioorg.2024.108119.

[17] El-Kashef DH, Sewilam HM. Empagliflozin mitigates methotrexate-induced hepatotoxicity: Targeting ASK-1/JNK/Caspase-3 pathway. International Immunopharmacology. 2023; 114: 109494. https://doi.org/10.1016/j.intimp.2022.109494.

[18] Wang HF, He YQ, Ke Z, Liang ZW, Zhou JH, Ni K, *et al*. STING signaling contributes to methotrexate-induced liver injury by regulating ferroptosis in mice. Ecotoxicology and Environmental Safety. 2024; 287: 117306. https://doi.org/10.1016/j.ecoenv.2024.117306.

[19] Wang Y, Feng X, Li Y, Niu S, Li J, Shi H, *et al*. Targeting inflammation and necroptosis in diabetic kidney disease: A novel approach via PPARα modulation. International Immunopharmacology. 2025; 154: 114562. https://doi.org/10.1016/j.intimp.2025.114562.

[20] Abdollah MRA, Aly MH, Wally ME, Sedky NK, Saadawy AH, Badr E, *et al*. Trimetazidine mitigates methotrexate-induced liver damage: Insights From biochemical, histological, and in silico analyses. Archiv Der Pharmazie. 2025; 358: e2400726. https://doi.org/10.1002/ardp.202400726.

[21] Du J, Zou Q, Shen Y, Ren Q, Zhang Q, Zhao Q, *et al*. Monotropein mitigates methotrexate-induced liver injury by activating autophagy and inhibiting ferroptosis. Journal of Functional Foods. 2024; 121: 106413. https://doi.org/10.1016/j.jff.2024.106413.

[22] Dogra A, Gupta D, Bag S, Ahmed I, Bhatt S, Nehra E, *et al*. Glabridin ameliorates methotrexate-induced liver injury via attenuation of oxidative stress, inflammation, and apoptosis. Life Sciences. 2021; 278: 119583. https://doi.org/10.1016/j.lfs.2021.119583.

[23] Li Z, Liu T, Feng Y, Tong Y, Jia Y, Wang C, *et al*. PPARγ Alleviates Sepsis-Induced Liver Injury by Inhibiting Hepatocyte Pyroptosis via Inhibition of the ROS/TXNIP/NLRP3 Signaling Pathway. Oxidative Medicine and Cellular Longevity. 2022; 2022: 1269747. https://doi.org/10.1155/2022/1269747.

[24] Abdelhamid AM, Elsheakh AR, Suddek GM, Abdelaziz RR. Telmisartan alleviates alcohol-induced liver injury by activation of PPAR-γ/ Nrf-2 crosstalk in mice. International Immunopharmacology. 2021; 99: 107963. https://doi.org/10.1016/j.intimp.2021.107963.

[25] Li Q, Zhang W, Cheng N, Zhu Y, Li H, Zhang S, *et al*. Pectolinarigenin ameliorates acetaminophen-induced acute liver injury via attenuating oxidative stress and inflammatory response in Nrf2 and PPARa dependent manners. Phytomedicine. 2023; 113: 154726. https://doi.org/10.1016/j.phymed.2023.154726.

[26] Wu ZF, Liu XY, Deng NH, Ren Z, Jiang ZS. Outlook of Ferroptosis-Targeted Lipid Peroxidation in Cardiovascular Disease. Current Medicinal Chemistry. 2023; 30: 3550–3561. https://doi.org/10.2174/0929867330666221111162905.

[27] Ma XH, Liu JHZ, Liu CY, Sun WY, Duan WJ, Wang G, *et al*. ALOX15-launched PUFA-phospholipids peroxidation increases the susceptibility of ferroptosis in ischemia-induced myocardial

damage. Signal Transduction and Targeted Therapy. 2022; 7: 288. https://doi.org/10.1038/s41392-022-01090-z.

[28] Ding K, Liu C, Li L, Yang M, Jiang N, Luo S, *et al*. Acyl-CoA synthase ACSL4: an essential target in ferroptosis and fatty acid metabolism. Chinese Medical Journal. 2023; 136: 2521–2537. https://doi.org/10.1097/CM9.0000000000002533.

[29] Ni HY, Yu L, Zhao XL, Wang LT, Zhao CJ, Huang H, *et al*. Seed oil of Rosa roxburghii Tratt against non-alcoholic fatty liver disease in vivo and in vitro through PPARα/PGC-1α-mediated mitochondrial oxidative metabolism. Phytomedicine. 2022; 98: 153919. https://doi.org/10.1016/j.phymed.2021.153919.

[30] Wang C, Li Z, Zhao B, Wu Y, Fu Y, Kang K, *et al*. PGC-1α Protects against Hepatic Ischemia Reperfusion Injury by Activating PPARα and PPARγ and Regulating ROS Production. Oxidative Medicine and Cellular Longevity. 2021; 2021: 6677955. https://doi.org/10.1155/2021/6677955.

[31] Pang J, Yin L, Jiang W, Wang H, Cheng Q, Jiang Z, *et al*. Sirt1-mediated deacetylation of PGC-1α alleviated hepatic steatosis in type 2 diabetes mellitus via improving mitochondrial fatty acid oxidation. Cellular Signalling. 2024; 124: 111478. https://doi.org/10.1016/j.cellsig.2024.111478.